The dynamical behavior of the earth's magnetosphere based on laboratory simulation

R. Rana[1], S. Minami[1], S. Takechi[1], A. I. Podgorny[2], and I. M. Podgorny[3]

[1]*Department of Electrical Engineering, Osaka City University, Osaka 558-0014, Japan*
[2]*P. N. Lebdev Physical Institute, Moscow, Russia*
[3]*Space Research Institute, Moscow, Russia*

(Received May 17, 2004; Revised September 17, 2004; Accepted September 24, 2004)

A laboratory simulation experiment was performed to observe the dynamical behavior of the earth's magnetosphere, based upon the earthward electric field measurement in the magnetotail. The simulation was examined to satisfy the MHD scaling laws. The earthward electric field, E_x, is the signature of the current density based on $j \times B$ force in the tail, described by Podgorny (1978). The effect of the solar wind dynamic pressure to the earthward electric field, E_x, was investigated. The solar wind density was changed while the other parameters were kept almost constant. It is found that the E_x is modulated by the change in the solar wind dynamic pressure. The result also shows that the current continued to flow in the near earth region even after the solar wind had stopped. This result shows a similar resemblance to that of the particle confinement in the radiation belt of the real magnetosphere.
Key words: Magnetosphere, solar wind, electric field, magnetic field, current sheet, field aligned current, plasma confinement.

1. Introduction

For an understanding of the auroral acceleration mechanism and substorm formation, it is important to know the magnetospheric current system. Laboratory experiments have been performed by many workers to investigate the magnetosphere phenomena using an intense plasma flow simulating the solar wind and a strong dipole magnetic field simulating the earth (Bostick *et al*., 1963; Cladis *et al*., 1964; Kawashima, 1964; Fukushima and Kawashima, 1964; Osborne *et al*., 1964; Podgorny, 1976; Birn *et al*., 1992). The configuration of the field line of the magnetosphere was measured by using a magnetic probe with a uniformly applied external magnetic field simulating the IMF by Podgorny (1976) and Baum and Bratenahl (1982). Minami *et al*. (1977) invented a small discharge electrode in order to map the magnetic field line configuration in the tail region. The more detailed experiments have been done by Minami and Takeya (1985); Minami *et al*., (1988b) and Minami (1994). Exact scaling of the simulation experiments of the magnetosphere is examined, based on Schindler's criterion (Shindler, 1969). These experiments have shown the existence of the open and closed magnetosphere. The simulation of the magnetosphere of other planets is also conducted based on the same technologies (Minami *et al*., 1990). The simulation of different space phenomena, other than earth's magnetosphere, has been performed by Minami *et al*. (1986, 1988a) and Minami (1994).

The earthward electric field, E_x, was first measured by Minami *et al*. (1993) in the laboratory. The E_x is generated due to Hall Effect because the $j \times B$ force is applied to the electrons and the electric field accelerates ions (Podgorny and Podgorny 1992).

The E_x is expressed by,

$$E_x = (J_y/ne)B_z \tag{1}$$

where:

$$J = nev \tag{2}$$

where n, e, v are carrier charge density, charge and velocity, respectively (Minami *et al*., 1993).

The experimental value of the E_x was measured by an electric double probe and the magnetic field was measured by a magnetic probe. The result of experiment showed that the E_x decreases gradually far from the earth because B_z component decreases gradually as shown in Eq. (1). The result by Minami *et al*. (1993) also confirmed that the dawn-dusk current is dominantly carried by electrons. If the current is carried by the ions then the polarity of y-component of tail electric field is completely reversed. The measured E_x in the current sheet is relatively accurate and valuable to imagine the distribution of the current, J, in the tail.

The FAC sheets are responsible for the energy transport to the ionosphere. Podgorny *et al*. (2003) shows that the FAC generator is the earthward electric field, E_x, in the magnetotail. B_y using the satellite measurements it is shown by Podgorny *et al*. (2003) that there are two sheets flowing away from the ionosphere at low latitude and flowing into the ionosphere at high latitude. The electric field between the two FAC sheets reaches the value of about 150 mV/m. The electric field is directed perpendicular to the FAC sheets. The connection of the FAC in ionosphere is described by Podgorny *et al*. (2003). They show that the FAC is generated in the magnetotail due to earthward electric field appearance.

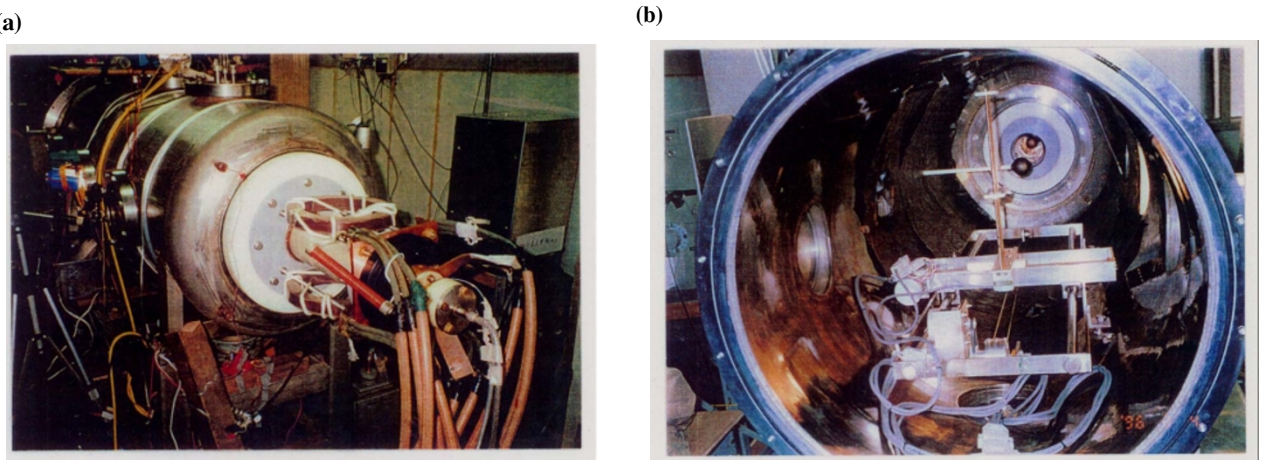

Fig. 1. (a) Outer view of the chamber. (b) Inner view of the chamber.

Table 1. The MHD scaling laws.

Parameters	Space	Experiment value	Scaled value
$\beta_d = 4\pi\rho_o\upsilon_o^2/B_o^2$	6–7	4–∞	6–7
$\beta_p = 4\pi k n_o T_o/B^2$	0.6	0.3	0.6
$R_m = 4\pi x_o \upsilon_o/\eta c^2$	$\sim 10^{12}$	10^3	$\gg 1$
$R_h = 4\pi x_o \upsilon_o n_o/cB_o$	$\sim 8 \times 10^3$	10	$\gg 1$

The electric field in MHD approximation is expressed by $E = -v \times B/c + j \times B/nec + \Delta p_e/ne$ (Podgorny *et al.*, 2003). The term pressure gradient, Δp_e, is negligible. During a substorm, plasma velocity, v, is directed to sun, and the electric field directed to sun can only be created by the Hall electric field $j \times B/nec$. The potential drop of this field is projected along the field line from the distance order of 20 R_E. Podgorny *et al.* (2003) described that the normal magnetic field B_n due to the existence of dipole geomagnetic field exists in entire current sheet in the magnetotail.

2. Experiment

To simulate the solar wind as a magnetohydrodynamic medium, it is necessary to eliminate electron-neutral collision effects and electron-ion collisions and to get a high magnetic Reynolds number, R_m. To get a fine structure of interaction between the simulated solar wind and the dipole magnetic field, the ion gyroradius must be small compared with the size of the earth's magnetosphere. In the experiment, the ion-neutral and ion-ion collisions have been reduced to make a collision-free solar wind. The condition for the ion-mean free paths in the laboratory simulation scaling laws by Baranov (1969) is too severe. Therefore the new entity has been added to calculate the ion-mean free path. (1) The simulated solar wind plasma is flowing at a very high speed and the residual neutral particles near the plasma gun expand slowly. During the solar wind and magnetosphere interaction of the duration 30 μsec, there is no neutrals particle from the gun in the experimental region. Therefore, electron-neutral collisions are neglected. (2) Due to the high plasma velocity, thermal velocity is replaced by the drift velocity of the simulated solar wind for the calculation of ion-mean free path. The new equation for effective ion-mean free path, λ_i^*, is given by,

$$\lambda_i^* = \nu_i/\upsilon_i \tag{3}$$

$$= \nu_i.T_i/4.78 \times 10^{-8} N_i Z^2 \ln\Lambda \tag{4}$$

where ν_i is the drift velocity. For the plasma density, N, $= 5 \times 10^{13}\text{cm}^{-3}$, the electron temperature, T, $= 10$ eV, and $\ln\Lambda$, $= 9$, the ion-mean free path, λ_i^*, is calculated as,

$$\lambda_i^* = 20 \text{ cm}. \tag{5}$$

Table 1 shows the laboratory and experimental simulation scaling values. The value of β_d is the solar wind dynamic beta, which is a function of the interplanetary magnetic field IMF B_o, applied perpendicular to the solar wind plasma flow. In this experiment, no IMF is applied in order to simplify the physics of the magnetosphere. Even without an IMF the shock of the magnetosphere is formed because of the existence of the earth's magnetic field. In this case, the magnetic field at the stagnation point, 100 G, is used as the effective value of IMF. The IMF is a second-order problem for this study. The value of β_p is the thermal beta which is a function of the ratio between plasma temperature and the IMF B_o (effective value of 100 G is used). The magnetic Reynolds number, R_m, is a function of plasma conductivity. For higher plasma conductivity, the ion gyroradius should be smaller than one. The value of R_h is the Hall parameters, which is a function of ion gyroradius and the size of the magnetosphere. For the fine structure of the magnetosphere, the ion gyroradius should be smaller than the earth's radius. This means that the value of R_h should be higher than one (Baranov, 1969). MHD scaling laws in Table 1 satisfies the scaling laws (Minami and Takeya, 1985).

Table 2. The parameters in space and experiment.

		Unit	Nature	Experiments
Plasma velocity near earth	v	cm/sec	3×10^7	3×10^7
Radius of magnetic vavity	R	cm	6×10^7	4
Magnetic field in IMF Bo	B_o	gamma	15	10^7
Plasma density	n	cm$^-$3	10	1×10^{13}
Electron temperature	T_e	eV	10	6
Ion temperature	T_i	eV	10	5
Ion gyro radius at shock front	L_i	cm	3×10^7	6.3×10^{-3}
Ion mean free path	λ_i^*	cm	1.3×10^5	20
Ion gyro frequency (shock front)	f_i	Hz	100	1.3×10^8
Plasma duration	Δt	sec	$\approx \infty$	3×10^{-5}

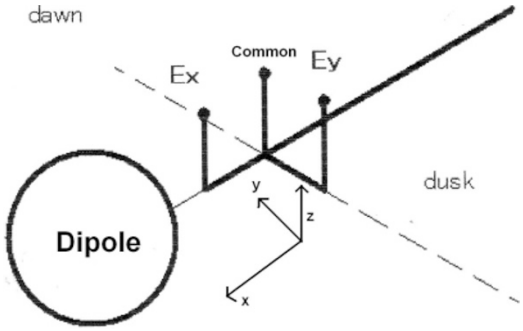

Fig. 2. A schematic illustration of the two double E-probes located along the sun-earth in the magnetotail.

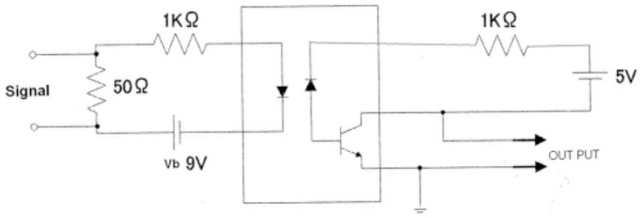

Fig. 3. The circuit of the photocoupler to measure the E_x and the E_y.

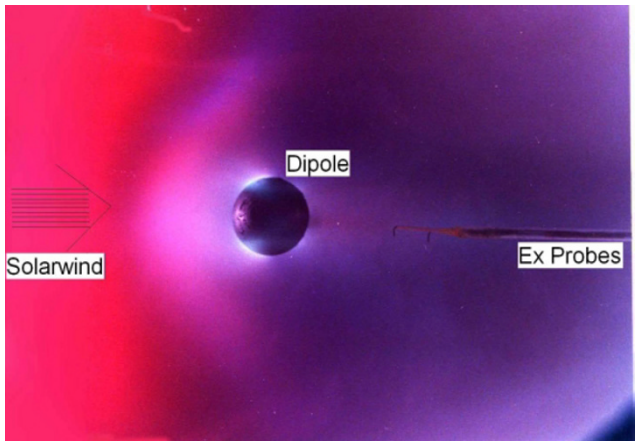

Fig. 4. The photograph of simulated magnetosphere. The simulated solar-wind plasma is coming from the left side and interacting with the dipole magnetic field.

Table 2 contains the laboratory simulation parameters which have been used in the experiment (Minami *et al.*, 1988).

The experiment was made by using a pulsed artificial hydrogen plasma flow to simulate the solar wind, produced by a coaxial plasma gun. Figure 1 is the experimental device, used in the simulation experiment. Figure 1(a) is the outer view of the chamber. The size of the vacuum chamber is 160 cm and 70 cm in length and in diameter respectively. Figure 1(b) is the inner view of the vacuum chamber, in which the dipole is inserted from the left side of the chamber. The applied voltage of the plasma gun, V_G, is 20 kV and the gun current, I_G, is 100 kA. A capacitor bank of capacity 6 μF has been used. The size of the simulated earth is 4 cm in diameter. A simulated dipole magnetic field is produced by the coil current, I_d, = 600 A. The surface of the dipole is conductively coated for the ionospheric current to flow. The I_d flows for about 1 ms, to create a magnetic field strength of 20 kG at the equator, which is long enough compared with the duration of the solar wind plasma. During the whole experiment, the base pressure was kept to 10^{-5} Torr.

The x and z component of electric field, E_x and E_y, are measured by two double E-probes located on the sun-earth line in the nightside magnetosphere as shown in Fig. 2. The probes are made of tungsten with a diameter of 1 mm and a length of 2 mm. The probes directed along x and y axis are represented as E_x and E_y respectively. The separation of the electrodes is 10 mm. In the laboratory experiment, the electron temperature has been measured along the tail and found that the value is almost constant of 5 eV. It can be said that the effect of electron temperature gradient between two points of the double probe is totally negligible for the electric field measurement. Figure 2 is a schematic illustration of the two double E-probes.

A high frequency response photocoupler with a light-emitting diode has been used to transfer the signal of E_x to eliminate a common mode noise. The overall frequency response of system is 1 μsec. Figure 3 is a diagram of the circuit.

Figure 4 shows a time exposure photograph of the simulated magnetosphere with the expanded luminosity in the magnetotail. The double E-probe is located in the nightside magnetosphere on the sun-earth line. The plasma flow sim-

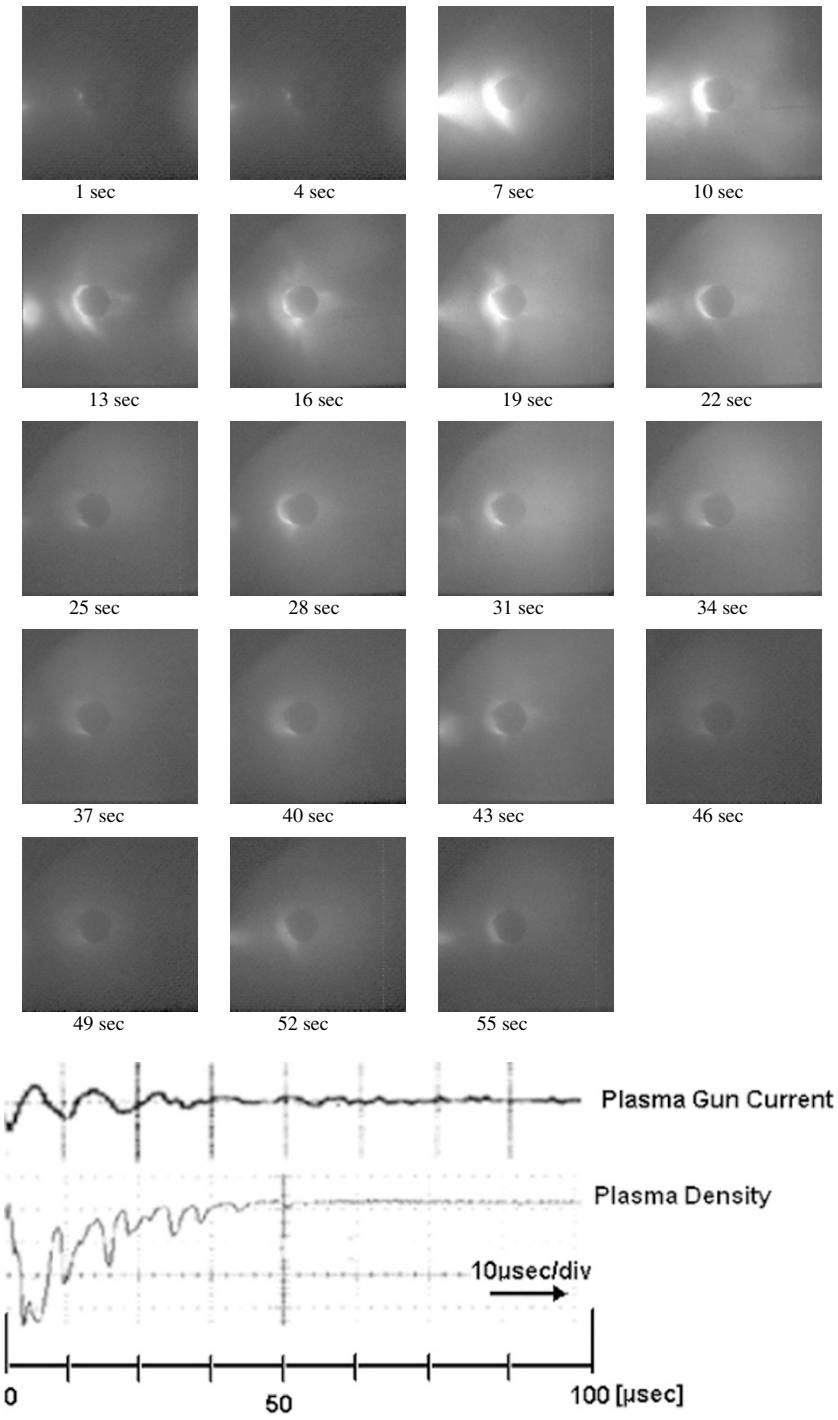

Fig. 5. A set of time-resolved photographs of the simulated solar wind interaction with the dipole magnetic field. The two waveform traces show the time variations of the plasma gun current and the solar wind plasma density. This plasma density was measured by a double probe.

ulating the solar wind comes from the left. The luminosity shows that bow-shock is created due to the super sonic flow interaction with the dipole magnetic field. The duration of the main pulsed plasma flow is 30 μsec. During the flow, in every 8 μsec the solar wind dynamic pressure is modulated by changing the gun current while the other parameters are kept almost constant. The characteristic time, T, for the plasma to pass through a dayside magnetosphere of 7 cm (corresponding to 10 R_E in space) is about 1 μsec (1 hour in space).

Figure 5 shows a set of time resolved-photographs of the interaction between the solar wind and the dipole magnetic field. The time difference between each frame photograph is 3 μsec. The each shutter time is 1 μsec. The simulated solar wind is coming from the left side of the photograph and is interacting with the dipole magnetic field in the centre. It can be seen from the photographs that the magnetosphere is created and modified due to the change in the dynamical pressure of the simulated solar wind plasma. The result shows that the magnetosphere shrinks and expands repeatedly, although the change of the configuration of the magnetosphere is faster than the framing period of 3 μs.

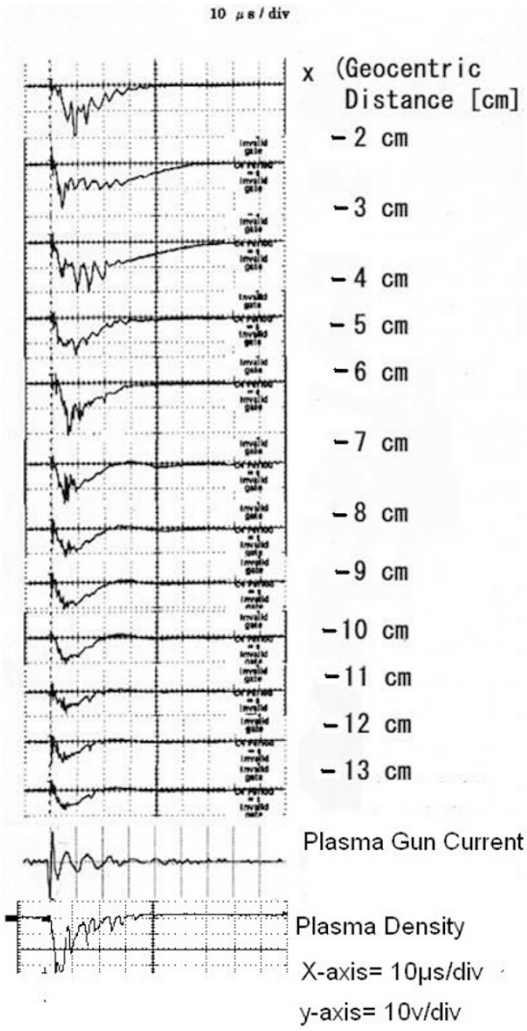

Fig. 6. The time variations of the earthward electric field, E_x, measured along sun-earth line in the nightside magnetosphere. The time variations of the plasma gun current and the solar wind plasma density are also shown.

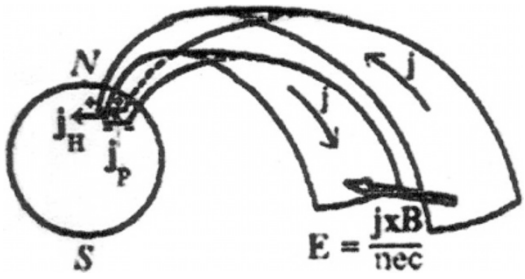

Fig. 7. A schematic illustration of the FAC circuit generated by Hall electric field in the tail current sheet (Podgorny *et al.*, 2003).

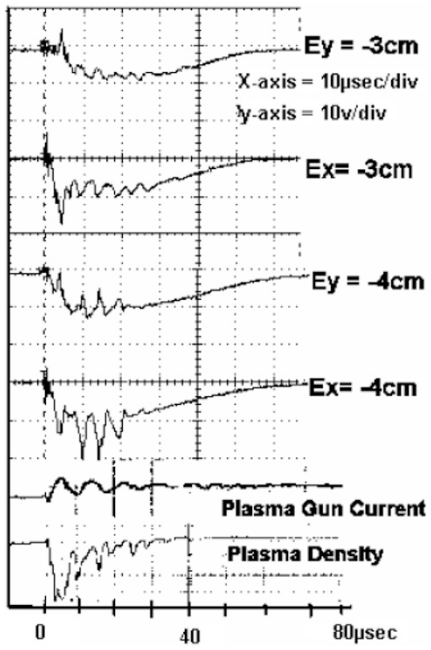

Fig. 8. The time variations of the measured E_x and E_y, at $x = -3$ cm and -4 cm, show the continuous flow of ring current in the magnetotail before and after the solar wind stopped. The time variations of the plasma gun current and the solar wind plasma density are also shown.

3. Results

3.1 Earthward electric field measurement

A double E-probe is used to measure the E_x. Figure 6 shows time variation of the E_x during the changes in the solar wind dynamic pressure. The main plasma gun current, and the solar wind density, measured on sun-earth line off the dipole, are also shown in Fig. 6. The E_x has been measured along the sun-earth line from $x = -2$ cm to $x = -13$ cm in the magnetotail. In the region between $x = -7$ cm and $x = -13$ cm, modulation of the E_x is weak compared with the modulation of E_x in the near-earth magnetotail region. The Eq. (1) shows that the E_x is a function of $j \times B$ force. The $j \times B$ force accelerates the plasma along the tail to the earth. The value B in Eq. (1) corresponds to the normal component of magnetic field, B_n, described by Podgorny *et al.* (2003). The B_n component is responsible for the earthward electric field, E_x, generation. The change in solar wind dynamic pressure strongly modulates the B_n component strength. In the near earth region, the $j \times B$ force strongly modulates due to the change in B_n component which results in the strong modulation of earthward electric field, E_x, generation. However, in the far-earth region, the strength of B_n component is weak therefore the $j \times B$ force decreases gradually and the E_x modulation decreases.

Figure 7 is a schematic illustration of the FAC structure (Podgorny *et al.*, 2003). The current flows along the dawn-dusk direction and closed FAC. The E_x causes charged particles to flow along the field lines. The field line structure described by Podgorny *et al.* (2003) may have some resemblance as of the experimental field lines.

3.2 Plasma confinement

Another significant result of the experiment is a rather long continuation of the plasma flow in the magnetosphere after the disappearance of solar wind. In Fig. 8, the time variation of E_x and E_y, measured at $x = -3$ cm and $x = -4$ cm, the plasma gun current and the solar wind density are shown. This result shows that the plasma has been trapped in this region, after the solar wind flow disappeared. It suggests that the ring current keeps flowing in this region. This region is similar to the Van-Allen belt in the real earth magnetotail located at a distance of 2 R_E. The time resolved visual plasma in Fig. 5 also shows the confinement of the plasma in

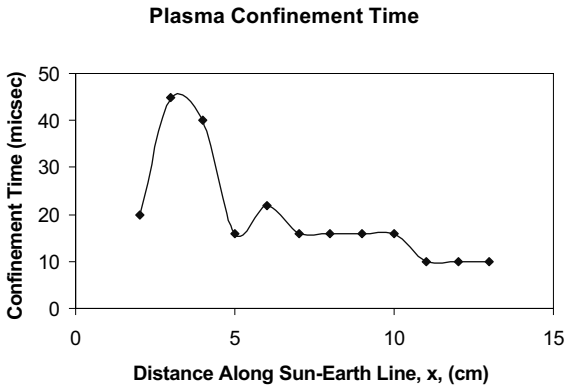

Fig. 9. Measured plasma confinement time at different positions along sun-earth line in the magnetotail.

the simulated magnetosphere, and the luminosity is present in the dipole magnetic field even after the solar wind flow disappears.

We calculated the plasma confinement time of the plasma current in the magnetotail using the Bohm diffusion time, t_B. The Bohm magnetic field diffusion coefficient, D_B, is given by

$$D_B = 1/16\,\mathrm{kT}_e/eB \tag{6}$$

and the plasma confinement time, t_B, is expressed as

$$t_B = R^2/2D_B \tag{7}$$

where R is the effective radius of the plasma column. The effective radius of the simulated ring current is regarded as about 1 cm. So for a magnetic field of 1 kG at the equator with the electron temperature, T_e, $=$ 10 eV and an effective radius, R, $=$ 1 cm, the value of Bohm magnetic field diffusion coefficient, D_B, is as follows;

$$D_B = 6 \times 10^4\ \mathrm{cm}^2 s^{-1} \tag{8}$$

and the plasma confinement time is calculated as:

$$t_B = 10\ \mu\mathrm{sec}. \tag{9}$$

Figure 9 is the measured plasma confinement time in the magnetotail at different positions, along sun-earth line. The confinement time is determined by the time when the E_x decreases to 10% of the maximum value at each position. It can be seen that the plasma confinement time decreases gradually as the position goes down to the tail. The confinement time at $x = -3$ cm and $x = -4$ cm is consistent with the time expressed by the Bohm diffusion time.

4. Conclusion

This experiment suggests that the dynamical behavior of the E_x in the tail is related to the structural change of the magnetosphere. Due to a change in the dynamical pressure of the solar wind, it is observed that the size of the magnetosphere shrinks and expands several times repeatedly. This modulation depth of about 50% is controlled by the change of the sheet current density in the tail. The current density is modulated by the shrinking of the magnetosphere.

The continuous flow of the tail current near the earth after the solarwind disappearance is related to the effective current confinement of the ring current particles. The confinement time is consistent with the predicted Bohm diffusion time of the plasma in the magnetic field. These results suggest some effective plasma confinement, as of the dipole configuration of the real magnetosphere. This result also supports the usefulness of the dipole confinement experiment for fusion research (Kesner *et al.*, 1998)

References

Baranov, P. J., Simulation of flow of interplanetary plasma past the magnetosphere of the earth or planets, *Cosmic Res.*, **7**, 98–104, 1969.

Baum, P. J. and A. Bartenahl, The laboratory magnetosphere, *Geophys. Res. Lett.*, **9**, 435–438, 1982.

Birn, J., G. Yur, H. U. Rahman, and S. Minami, On the termination of the closed field line region of the magnetotail, *J. Geophys. Res.*, **97**, 14883–14840, 1992.

Bostick, W. H., M. Brettschneider, and H. Byfield, Plasma flow around three-dimensional dipole, *J. Geophys. Res.*, **68**, 263–269, 1963.

Cladis, J. B., T. D. Miller, and J. R. Baskett, Interaction of supersonic plasma stream with a dipole magnetic field, *J. Geophys. Res.*, **69**, 463–469, 1964.

Fukushima, N. and N. Kawashima, Model experiments and neutral phenomena of interaction of solar plasma stream with geomagnetic field, Rep. Ionos, Space Res. Japan, 18, 4, 1964.

Kawashima, N., The interaction of plasma stream with three-dimensional magnetic dipole, *J. Phys. Soc.*, **18**, 59–64, 1964.

Kesner, J., L. Bromberg, D. Garnier, and M. Mauel, Plasma confinement in a magnetic dipole, ICP/09, 17th Fusion Energy Conference, Oct 19–24, 1998.

Minami, S., Effects of the local interstellar medium magnetic filed on the structure of the heliosphere: A laboratory simulation, *Geophys. Res. Lett.*, **21**, 81–84, 1994.

Minami, S. and Y. Takeya, Flow of artificial plasma in a simulated magnetosphere: Evidence of direct interplanetary magnetic field control of the magnetosphere, *J. Geophys. Res.*, **90**, 9503–9518, 1985.

Minami, S., Y. Hirose, and Y. Takeya, Simulation experiment of twined plasma produced by powered double probe in the tail region of the magnetosphere, Mem. of Fac. of Eng. Osaka City Uni., 18, 27–36, 1977.

Minami, S., P. J. Baum, G. Kamin, and R. S. White, Laboratory formation of a simulated comet, *Geophys. Res. Lett.*, **13**, 884–887, 1986.

Minami, S., P. J. Baum, G. Kamin, and R. S. White, Laboratory comet simulation experiments, in *Laboratory and Space Plasmas,* edited by H. Kikuchi, 621 pp., Springer Verlag, New York, 1988a.

Minami, S., P. J. Baum, G. Kamin, and Y. Takeya, Laboratory behavior of a plasma plume injected into the magnetized plasma flow, *J. Geomag. Geoelectr.*, **40**, 1283–1302, 1988b.

Minami, S., K. Hashimoto, and Y. Takeya, Dipole tilt angle effect on the magnetosphere of Neptune—a laboratory simulation, *Geophys. Res. Lett.*, **17**, 896–899, 1990.

Minami, S., I. M. Podgorny, and A. I. Podgorny, Laboratory evidence of Earthward electric field in the magnetotail current Sheet, *Geophys. Res. Lett.*, **20**(1), 9–12, 1993.

Osborne, F. J. F., M. P. Bachynski, and J. V. Gore, Laboratory studies of the variation of the magnetosphere, *J. Geophys. Res.*, **69**, 4441, 1964.

Podgorny, I. M., Laboratory experiments (Plasma intrusion into the magnetic field), Space Research Institute, Rep. Pr.-225, 1976.

Podgorny, I. M., Current sheet formation, in *Fundamental of Cosmic Physics,* 4, pp. 1, 1978.

Podgorny, A. I. and I. M. Podgorny, A solar flare model including the formation and destruction of the current sheet in the corona, *Solar Phys.*, **139**, 125–145, 1992.

Podgorny, I. M., A. I. Podgorny, S. Minami, and R. Rana, The mechanism of energy release and field-aligned current during the substorms and solar flares, *Advances in Polar Upper Atmosphere Research,* **17**, 77–83, 2003.

Schindler, K., Laboratory experiments related to the solarwind and the magnetosphere, *Rev. of Geophys.*, **7**(1,2), 51–75, 1969.

R. Rana (e-mail: rana@em.elec.eng.osaka-cu.ac.jp), S. Minami, S. Takechi, A. I. Podgorny, and I. M. Podgorny